Quantifying perpendicular magnetic anisotropy at the Fe-MgO(001) interface

C.-H. Lambert,[1,2] A. Rajanikanth,[1] T. Hauet,[1] S. Mangin,[1] E. E. Fullerton,[2] and S. Andrieu[1,a)]
[1]*Institut Jean Lamour, UMR CNRS 7198, Université de Lorraine, 54506 Vandoeuvre lès Nancy, France*
[2]*Center of Magnetic Recording Research, University of California, San Diego, California 92093-0401, USA*

(Received 13 January 2013; accepted 11 March 2013; published online 29 March 2013)

We show that Fe-MgO interfaces possess strong perpendicular magnetic anisotropy of 1.0 ± 0.1 erg/cm^2 in fully epitaxial MgO/V/Fe/MgO(001) and MgO/Cr/Fe/MgO(001) heterostructures. The sign and amplitude of the total anisotropy are quantified as a function of Fe thickness using magnetometry and ferromagnetic resonance. There is a transition from out-of-plane to in-plane anisotropy for 6 Fe monolayers in V/Fe/MgO and only 4 monolayers in Cr/Fe/MgO. A detailed study of the Fe magnetization and effective anisotropy in both systems explains this difference and quantifies the Fe-MgO interface anisotropy. © *2013 American Institute of Physics*. [http://dx.doi.org/10.1063/1.4798291]

The implementation of films with perpendicular magnetic anisotropy (PMA) enables a broad range of magnetic nanotechnologies. PMA materials have been implemented in hard disk drives for more than a decade delaying the onset of the superparamagnetic limit and are also the basis for prototype bit-patterned media.[1] There is current interest in integrating PMA materials into spin transfer torque magnetic random access memory (STT-MRAM) as PMA materials provide a pathway to low critical current and high thermal stability.[2]

Perpendicular STT-MRAM devices need to combine large tunnel magnetoresistance (TMR) to read the information and large spin torque efficiency to switch magnetization with a polarised current. This has been largely achieved through the discovery of PMA in CoFeB/MgO/CoFeB magnetic tunnel junctions.[3–7] It has further been shown that the PMA can be tuned by the application of a voltage.[8–12] Theoretical analyses highlight different possible mechanism that would lead to PMA and generally involves band hybridization, spin-orbit coupling splitting or strain.[13–15] Particularly, Yang *et al.* attributed the PMA to a combination of two factors: overlap between O-pz and transition metal dz^2 orbitals, as well as degeneracy lift of out-of-plane 3d orbitals induced by spin-orbit coupling.[14] In addition, He and Chen have shown that the lattice mismatch between MgO and FeCo could also induce an additional PMA.[15] Predicted PMA amplitudes can reach 1.46 erg/cm^2 in Ref. 14 and 1.9 erg/cm^2 in Ref. 15 per Fe-MgO interface. Such values are more than 2 times larger than the value obtained for other interface-induced PMA like in Co/Pd, Co/Pt, Fe/Ag, Fe/Au, or Co/Ni.[16]

Many recent experimental reports deal with tuning PMA and demonstrating the role of Fe_xCo_{1-x}-MgO interface. Effect of buffer/cap, inserted Mg layer, MgO thickness, Fe_xCo_{1-x} concentration, CoFeB annealing,[3–7] and electric charges[17,18] has been investigated. Besides, similar researches have focused on Co/AlO_x interfaces[19,20] and FePd/MgO.[21] Most of these recent experimental results confirm that Fe_xCo_{1-x}/MgO provides an anisotropy that is perpendicular to the interface. However, the amplitude of PMA anisotropy found in the literature shows a large spectrum of PMA amplitude[6–9,17,18] and the largest values stay much below the theoretical predictions.[13–15] One could argue that CoFeB-MgO interfaces obtained by sputtering exhibit structural defects whereas perfect interfaces are generally assumed in calculations. However even in molecular beam epitaxy (MBE) grown Au/Fe/MgO system, the Fe/MgO magnetic anisotropy is found to be much lower than the Au/Fe one, i.e., lower than 0.5 erg/cm^2.[5,9,10]

In this letter, we present a careful study of the magnetic features of MBE-grown single-crystal MgO/V/Fe/MgO (001) and MgO/Cr/Fe/MgO (001) heterostructures. Magnetization and magnetic anisotropies are measured by different techniques including magneto-optic Kerr effect (MOKE), ferromagnetic resonance (FMR), and magnetometry for Fe thickness ranging from 5 to 12 monoatomic layers (MLs). By considering the contributions of the Fe magneto-crystalline and shape anisotropies, and the V-Fe, Cr-Fe and Fe-MgO interfaces anisotropies, we can quantify the Fe-MgO interface anisotropy and compare to existing experimental and theoretical results.

The samples were grown on single-crystal MgO (100) substrate using MBE with a base-pressure lower than 10^{-10} Torr. The V or Cr buffer layers were deposited at room temperature (RT) and then annealed at 600 °C. An Fe wedge was then grown on the V or Cr buffer layers and covered with a 6-ML (1.2 nm) MgO(001) film. The typical stacking of a sample is thus V or Cr(10 nm)/Fe(t_{Fe})/MgO(1.2 nm) where the Fe thickness t_{Fe} is varied from 5 to 12 MLs in 1 ML steps. Fe was deposited at RT with no further annealing and capped with MgO also at RT. The epitaxial relationship, growth mode, number of deposited MLs, and surface flatness were controlled *in situ* using reflection high energy electron diffraction (RHEED). Figures 1(a) and 1(b) show RHEED intensity oscillations recorded during the growth of Fe on Cr and V, respectively. The oscillation period corresponds to 1 ML, which allows accurate control of t_{Fe} and demonstrates layer-by-layer growth and a low surface roughness. The RHEED patterns in the insets confirm the (001) crystalline order for the Cr and V buffer layers and Fe magnetic layers.

Figure 2 shows magnetization curves measured using a Quantum Design SQUID-VSM on both V/Fe(5–7 MLs)/MgO

a)Author to whom correspondence should be addressed. Electronic mail: stephane.andrieu@ijl.nancy-universite.fr.

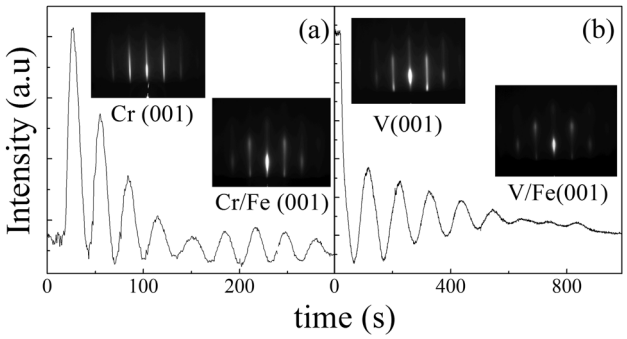

FIG. 1. RHEED intensity oscillations recorded during the growth of Fe on Cr(001) (a) and V(001) (b), respectively. In inset, RHEED patterns of V and Cr (001) buffer layers are shown, as well as Cr/Fe(8 MLs) and V/Fe(8 MLs).

and Cr/Fe(3–5 MLs)/MgO systems for both in-plane and out-of-plane applied magnetic fields. For the thinnest Fe layers, we observed square out-of-plane loops indicating PMA for the system. For the V/Fe/MgO(001) wedge (Figs. 2(a)–2(c)), the preferential magnetization direction moves from out-of-plane to in-plane as Fe thickness increases from 5 to 7 MLs. In contrast for the Cr/Fe/MgO(001) wedge (Figs. 2(d)–2(f)), this transition occurs for 3–5 ML. Considering that the origin of the PMA in such thin Fe layers is thought to be primarily due to the Fe-MgO interface anisotropy, these results clearly show additional contributing factors.

This apparent contradiction results from the difference in the magnetization of the Fe layers in both systems. The measured areal magnetic moment (i.e., M divided by sample area in erg/cm^2) should increase linearly with the Fe thickness. If the Fe atomic moment is the same for all Fe atoms in the film, the $M_{/area}(t_{Fe})$ should be a straight line passing through 0, with a slope equal to the bulk Fe magnetization (about 1715 emu/cm^3). It is indeed observed in the Cr/Fe/MgO system (see inset of Fig. 3). This means that the Fe atomic moment is similar in the whole film, and consequently also at the Cr/Fe interface. The V/Fe/MgO system does not behave the same way (inset in Fig. 3). If the $M(t_{Fe})$ slope in V/Fe/MgO is similar to the slope observed in Cr/Fe/MgO (corresponding to a magnetization of 1680 ± 50 emu/cm^3 which is close to the bulk Fe value), the straight line fit clearly crosses zero for 0.3 nm. Such results suggest that there is a deadlayer thickness $t_{dl} = 0.3$ nm indicating 2 dead magnetic MLs in our V/Fe/MgO samples. This behavior is in fact not surprising since a reduction of Fe magnetization at the interface with V is known and has been explained by roughness, charge transfer, and anti-parallel polarization of the V.[22,23] An oxygen contamination of the starting V(001) surface should also contribute to these magnetic dead layers in Fe grown at RT.[24]

The effective anisotropy constant K_{eff} was extracted from the area between the out-of-plane and in-plane loops in one of the hysteresis quadrants. The results are shown in Fig. 3 where we plot the result for the magnetic thickness $(t_{Fe} - t_{dl})$. We also measured the V/Fe/MgO wedge samples for t_{Fe} ranging from 7 to 12 MLs using MOKE and FMR. The FMR measurements used a coplanar waveguide connected to a vector network analyzer to both generate and record the signal. The external DC magnetic field was applied in-plane. Figure 4 shows the typical FMR profiles obtained for in-plane magnetized samples. Shift in the field resonance with in-plane applied field gives access to the effective anisotropy through the relation $\omega_0 = \gamma\,[H_{ip}\,(H_{ip} + H_{Keff})]^{1/2}$ where ω_0 is the frequency at resonance, γ is the magneto-mechanical ratio for an electron spin, H_{ip} is the strength of the static applied magnetic field, and H_{Keff} is the effective anisotropy field of the sample $H_{Keff} = 2K_{eff}/M_s$ (Ref. 25) (we ignore here the small Fe cubic anisotropy). MOKE experiments were performed with an applied field perpendicular to the sample plane. For all samples, typical hard axis loops were recorded and anisotropy fields were extracted assuming a square in-plane loop. The results for various thicknesses are also shown in Fig. 3.

The values of effective anisotropies K_{eff} extracted from SQUID-VSM, FMR, and MOKE experiments are plotted in

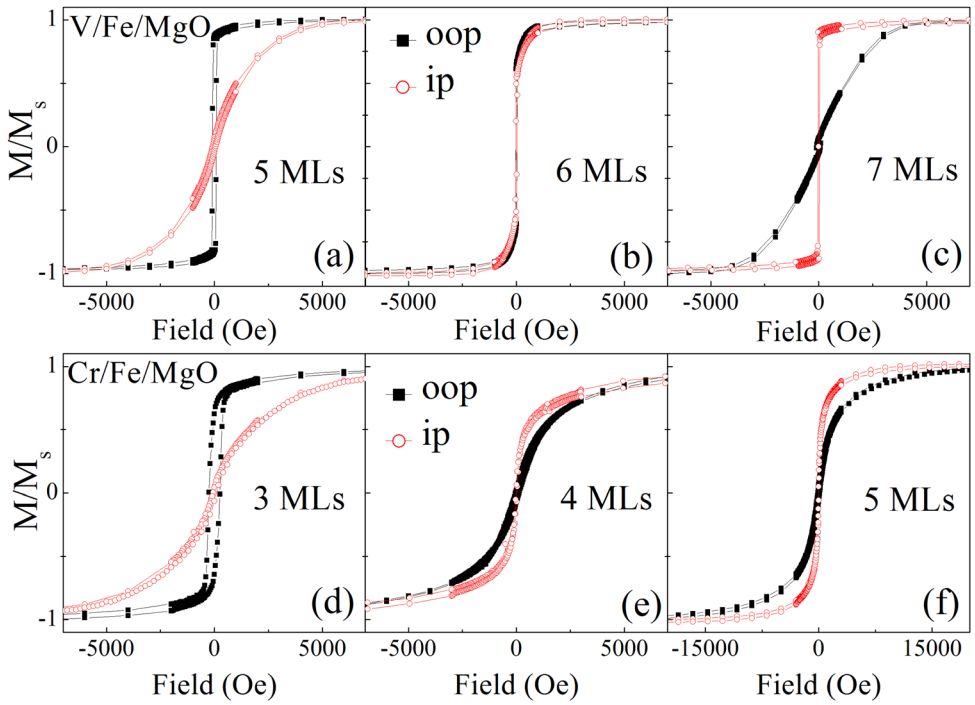

FIG. 2. Room temperature normalized magnetization as a function of magnetic field applied out-of-plane (OOP-black squares) and in the film plane (IP-red open circles), measured on V/Fe/MgO sample with t_{Fe} set to (a) 5 MLs, (b) 6 MLs and (c) 7 MLs and on Cr/Fe/MgO with t_{Fe} set to (d) 3 MLs, (e) 4 MLs and (f) 5 MLs.

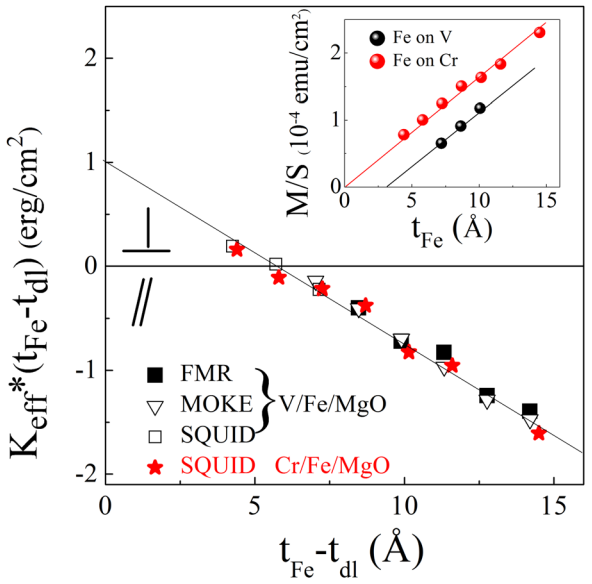

FIG. 3. Effective anisotropy constant K_{eff} times t_{Fe}-t_{dl} as a function of t_{Fe}-t_{dl} deduced from SQUID-VSM, FMR, and MOKE measurements at RT for both V/Fe/MgO and Cr/Fe/MgO systems. The line is a fit using Eq. (2). In inset are plotted the areal magnetization versus Fe thickness, showing that $t_{dl} = 0$ for Fe on Cr and $t_{dl} = 3$ Å for Fe on V.

Fig. 3 versus the active Fe thickness corrected from the dead layers at Fe/V interface. The unique linear variation confirms the good agreement between the results obtained from the different techniques. This behavior is usually explained writing the effective anisotropy as the sum of the different anisotropy contributions as[16] (here in CGS unity)

$$K_{eff} = K_V + \frac{K_s}{t} - 2\pi M_s^2, \tag{1}$$

where K_v is the magnetic volume anisotropy and K_s is the interfaces anisotropy acting in the Fe layer. The $-2\pi M_s^2$ term comes from the shape anisotropy for a thin film. The negative sign shows that this anisotropy term tends to align the magnetization in the film plane. The thickness t is the thickness of the film, but here we should take into account

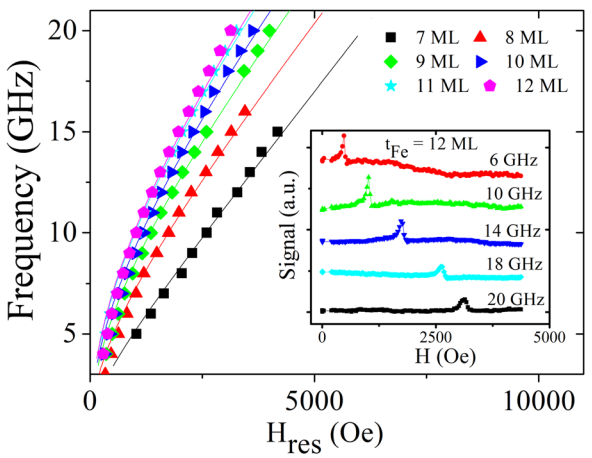

FIG. 4. FMR resonance field plotted versus DC magnetic field frequency (points) and simulations (lines) performed on V/Fe/MgO wedge with $t_{Fe} = 7$, 8, 9, 10, 11, and 12 MLs. In inset, typical FMR responses versus field for $t_{Fe} = 12$ MLs for several excitation frequencies of the in-plane applied DC field.

only the active magnetic layers, that is $t = t_{Fe} - t_{dl}$. We thus get the linear relationship

$$K_{eff}(t_{Fe}-t_{dl}) = (K_V - 2\pi M_s^2)(t_{Fe}-t_{dl}) + K_s, \tag{2}$$

where $t_{dl} = 2$ MLs for Fe on V and $t_{dl} = 0$ for Fe on Cr. We can go further by looking in details at the volume and interface anisotropy contributions. From the slope of the experimental curve in Fig. 3, we can extract a value of the volume anisotropy $K_v - 2\pi M_s^2 = -1.78 \times 10^7$ erg/cm^3. By taking into account $M_s = 1680 \pm 50$ emu/cm^3, the calculated shape anisotropy term is $2\pi M_s^2 = 1.8 \times 10^7$ erg/cm^3. Therefore, we can conclude that K_V is small as compared with shape anisotropy. Indeed, volume anisotropy of cubic Fe is usually of the order of few 10^5 erg/cm^3 (Refs. 26 and 27) and magneto-elastic contributions are expected to be small. It should be pointed out that a magneto-elastic contribution in K_v should also be taken into account in the case of strained epitaxial thin films. This contribution is very small in Cr/Fe/MgO since the Cr/Fe misfit is around 0.6%. But the misfit is much larger in V/Fe, around 5.6%. Consequently, if the Fe growth on V is pseudomorphic, the magnetoelastic anisotropy should be non-negligible. However, we have shown in a previous study[28] that the critical thickness for plastic relaxation during Fe growth on V at RT in our MBE system is lower than 1 ML. This means that Fe layer relaxes to its stable bcc structure, leading to small magnetoelastic anisotropy. As a consequence, the volume anisotropy originates mostly from the demagnetization term.

There are two contributions in K_s, one coming from the V-Fe or Cr-Fe interfaces, the other from the Fe-MgO one. V/Fe/V superlattices have been heavily studied in the past and in-plane anisotropy has always been reported for Fe thickness as low as 3 MLs.[29–31] At low temperatures, Anisimov *et al.* found positive interface anisotropy of the order of few merg/cm^2 that monotonically disappears as the temperature increases to RT.[29] The value of K_s at Cr/Fe interface has been measured only once in Ref. 32 as $+0.19$ erg/cm^2. To summarize, both data for Fe on Cr and on V in Fig. 3 are well described by Eq. (2) considering a negligible K_v contribution. Therefore only K_s is an unknown parameter in Eq. (2) and the accuracy on this extracted K_s value is very good yielding a value of 1.0 ± 0.1 erg/cm^2. As the V-Fe interface anisotropy is very small, this means that this K_s value comes from the Fe/MgO interface. We should however observe a slightly higher total K_s in Cr/Fe/MgO since the Cr/Fe interface contribution is not negligible when compared to the extracted Fe-MgO one.

The extracted K_s value for Fe/MgO interface is larger than the value obtained in MBE-grown Au/Fe_xCo_{1-x}/MgO (<0.5 erg/cm^2)[6,16,18] but smaller than in tuned CoFeB/MgO interfaces (1.6 erg/cm^2).[7] Such a dispersion of the K_s values is in fact not surprising since K_s determination by analyzing K_{eff} may depend on subtleties that mainly come from samples preparation. This is particularly true for Fe on V here: Plotting $K_{eff}t_{Fe}$ versus t_{Fe} (that is ignoring the dead layers) leads to a K_s two times larger. Finally, we observe a K_s smaller than calculated ones.[14,15] One possible explanation may be the level of oxidation of Fe in contact with MgO as pointed out in Ref. 14, but we never observed such an effect in our samples.[33,34] However, other defects like steps, kinks, and vacancies present

in real systems are difficult to take into account in calculations and may decrease this interface anisotropy.

In summary, detailed analysis of magnetic properties (magnetization, effective anisotropy) allows us to enlighten the origin of PMA in V/Fe/MgO(001) and Cr/Fe/MgO(001) epitaxial layers. The Fe thickness limit for getting PMA is found to be different in both systems (below 6 MLs in V/Fe/MgO and 4 MLs in Cr/Fe/MgO). This is explained by the occurrence of 2 MLs magnetic dead layers in Fe on V that does not exist on Cr. For a given Fe thickness, the shape anisotropy is thus smaller in V/Fe than in Cr/Fe whereas the Fe/MgO interface anisotropy is found to be similar for both systems. This work allows an accurate and robust determination of the Fe/MgO interface anisotropy $K_s = 1.0 \pm 0.1$ erg/cm^2 (mJ/m^2) responsible for PMA. Such a high K_s (around 2 times larger than in the low spin-orbit prototype Co/Ni(111) system[35]) is very promising for further use in STT-RAM and spintronic systems.

This work was supported by the French Agence Nationale de la Recherche, ANR-10-BLANC-1005 "Friends," ANR-2010-BLANC-1006 "Elecmade," and work at UCSD was supported by NSF Award # 1002147. It was also supported by The Partner University Fund "Novel Magnetic Materials for Spin Torque Physics" as well as the European Project (OP2M FP7-IOF-2011-298060) and the Region Lorraine.

[1]O. Ozatay, P. G. Mather, J. U. Thiele, T. Hauet, and P. M. Braganca, "Spin-based data storage," in *Nanofabrication and Devices of Comprehensive Nanoscience and Nanotechnology*, edited by D. Andrews, G. Scholes, and G. Wiederrecht (Elsevier, London, 2010), Vol. 4, pp. 561–614.
[2]S. Mangin, D. Ravelosona, J. A. Katine, M. J. Carey, B. D. Terris, and E. E. Fullerton, Nature Mater. **5**, 210 (2006).
[3]S. Ikeda, K. Miura, H. Yamamoto, K. Mizunuma, H. D. Gran, M. Endo, S. Kanai, J. Hayakawa, F. Matsukura, and H. Ohno, Nature Mater. **9**, 721 (2010).
[4]J. H. Jung, S. H. Lim, and S. R. Lee, Appl. Phys. Lett. **96**, 042503 (2010).
[5]K. Lee, J. J. Sapan, S. H. Kang, and E. E. Fullerton, J. Appl. Phys. **109**, 123910 (2011).
[6]M. Yamanouchi, R. Koizumi, S. Ikeda, H. Sato, K. Mizunuma, K. Miura, H. D. Gan, F. Matsukura, and H. Ohno, J. Appl. Phys. **109**, 07C712 (2011).
[7]Q. L. Ma, S. Lihama, T. Kubota, X. M. Zhang, S. Mizukami, Y. Ando, and T. Miyazaki, Appl. Phys. Lett. **101**, 122414 (2012).
[8]M. Weisheit, S. Fähler, A. Marty, Y. Souche, C. Poinsignon, and D. Givord, Science **315**, 349 (2007).
[9]Y. Shiota, T. Maruyama, T. Nozaki, T. Shinjo, M. Shiraishi, and Y. Suzuki, Appl. Phys. Express **2**, 063001 (2009).
[10]T. Maruyama, Y. Shiota, T. Nozaki, K. Ohta, N. Toda, M. Mizuguchi, A. A. Tulapurka, T. Shinjo, M. Shiraishi, S. Mizukami, Y. Ando, and Y. Suzuki, Nat. Nanotech. **4**, 158 (2009).
[11]K. Nakamura, R. Shimabukuro, Y. Fujiwara, T. Akiyama, T. Ito, and A. J. Freeman, Phys. Rev. Lett. **102**, 187201 (2009).
[12]W.-G. Wang, M. Li, S. Hageman, and C. L. Chien, Nature Mater. **11**, 64 (2012).
[13]M. K. Niranjan, C.-G. Duan, S. S. Jaswal, and E. Y. Tsymbal, Appl. Phys. Lett. **96**, 222504 (2010).
[14]H. X. Yang, M. Chshiev, B. Dieny, J. H. Lee, A. Manchon, and K. H. Shin, Phys. Rev. B **84**, 054401 (2011).
[15]K. H. He and S. J. Chen, J. Appl. Phys. **111**, 07C109 (2012).
[16]M. T. Johnson, P. J. H. Bloemen, F. J. A. den Broeder, and J. J. de Vries, Rep. Prog. Phys. **59**, 1409–1458 (1996).
[17]Y. Shiota, T. Nozaki, F. Bonell, S. Murakami, T. Shinjo, and Y. Suzuki, Nature Mater. **11**, 39 (2012).
[18]T. Nozaki, Y. Shiota, M. Shiraishi, T. Shinjo, and Y. Suzuki, Appl. Phys. Lett. **96**, 022506 (2010).
[19]A. Manchon, C. Ducruet, L. Lombard, S. Auffret, B. Rodmacq, B. Dieny, S. Pizzini, J. Vogel, V. Uhlíř, M. Hochstrasser, and G. Panaccione, J. Appl. Phys. **104**, 043914 (2008).
[20]D. Lacour, M. Hehn, M. Alnot, F. Montaigne, F. Greullet, G. Lengaigne, O. Lenoble, S. Robert, and A. Schuhl, Appl. Phys. Lett. **90**, 192506 (2007).
[21]F. Bonell, S. Murakami, Y. Shiota, T. Nozaki, T. Shinjo, and Y. Suzuki, Appl. Phys. Lett. **98**, 232510 (2011).
[22]J. Izquierdo, R. Robles, A. Vega, M. Talanana, and C. Demangeat, Phys. Rev. B **64**, 060404(R) (2001).
[23]M. Sicot, S. Andrieu, P. Turban, Y. Fagot-Revurat, H. Cercellier, A. Tagliaferri, C. De Nadai, N. B. Brookes, F. Bertran, and F. Fortuna, Phys. Rev. B **68**, 184406 (2003).
[24]F. Dulot, P. Turban, B. Kierren, J. Eugène, M. Alnot, and S. Andrieu, Surf. Sci. **473**, 172 (2001).
[25]C. Kittel, Phys. Rev. **73**, 155 (1948).
[26]C. D. Graham, Phys. Rev. **112**, 1117 (1958).
[27]D. Sander, J. Phys.: Condens. Matter **16**, 603 (2004).
[28]P. Turban, L. Hennet, and S. Andrieu, Surf. Sci. **446**, 241 (2000).
[29]A. N. Anisimov, M. Farle, P. Poulopoulos, W. Platow, K. Baberschke, P. Isberg, R. Wäppling, A. M. N. Niklasson, and O. Eriksson, Phys. Rev. Lett. **82**, 2390 (1999).
[30]H. Fritzche, T. Nawrath, H. Maletta, and H. Lauter, Physica B **241–243**, 707 (1997).
[31]A. Broddefalka P. Nordblada, P. Blomqvist, P. Isberg, R. Wappling, O. Le Bacq, and O. Eriksson, J. Magn. Magn. Mater. **241**, 260 (2002).
[32]A. Macedo Texeira, C. A. Ramos, A. A. R. Fernandes, and E. E. Fullerton, J. Magn. Magn. Mater. **226–230**(2), 1788 (2001).
[33]V. Serin, S. Andrieu, R. Serra, F. Bonell, C. Tiusan, L. Calmels, M. Varela, S. J. Pennycook, E. Snoeck, M. Walls, and C. Colliex, Phys. Rev. B **79**, 144413 (2009).
[34]F. Bonell, S. Andrieu, A. M. Bataille, C. Tiusan, and G. Lengaigne, Phys. Rev. B **79**, 224405 (2009).
[35]M. Gottwald, S. Andrieu, F. Gimbert, E. Shipton, L. Calmels, C. Magen, E. Snoeck, M. Liberati, T. Hauet, E. Arenholz, S. Mangin, and E. E. Fullerton, Phys. Rev. B **86**, 014425 (2012), and references therein.